SPECIAL PROJECT PROGRESS REPORT

All the following mandatory information needs to be provided. The length should *reflect the complexity and duration* of the project.

Reporting year

2019

Project Title:

Deep Vertical Propagation of Internal Gravity Waves

Computer Project Account:

SPDESCAN

Principal Investigator(s):

Dr. Andreas Dörnbrack
Dr. Sonja Gisinger
Dr. Klaus-Peter Hoinka

Affiliation:

DLR Oberpfaffenhofen
Institut für Physik der Atmosphäre
Münchener Str. 20

D – 82230 WESSLING

Germany

Name of ECMWF scientist(s) collaborating to the project
(if applicable)

Dr. Nils Wedi
Dr. Christian Kühnlein
Dr. Piotr K Smolarkiewicz

Start date of the project:

1 January 2018

Expected end date:

2020

Computer resources allocated/used for the current year and the previous one

(if applicable)
Please answer for all project resources

		Previous year		Current year	
		Allocated	Used	Allocated	Used
High Performance Computing Facility	(units)	500000	500000	500000	260000
Data storage capacity	(Gbytes)	80	80	80	80

Summary of project objectives

During the recent years, ground-based and airborne Rayleigh lidar measurements of temperature perturbations in the middle atmosphere show gravity wave activity covering a large spectrum of frequencies and vertical and horizontal wavelengths. An understanding of the different wave modes in the middle atmosphere is still lacking. Especially, the link of the observed gravity wave activity to possible sources in the troposphere as well as in the stratosphere is difficult to establish as 3D data of wind and temperature in high spatial and temporal resolution are missing. Therefore, the integrated forecast system (IFS) of the ECMWF will serve to fill this gap by providing these data globally. One example of the feasibility to simulate stratospheric gravity waves is documented in Dörnbrack et al. (2017). Idealized numerical simulations will complement the combined analysis of data and IFS output. Thus, the project is based on three ingredients.

Summary of problems encountered

no problems encountered

Summary of plans for the continuation of the project (10 lines max)

We continue like planned and outlined in the proposal.

List of publications/reports from the project with complete references

1. Bramberger, M., A. Dörnbrack, H. Wilms, S. Gemsa, K. Raynor, and R. Sharman, 2018: Vertically Propagating Mountain Waves — A Hazard for High-Flying Aircraft?.*J. Appl. Meteor. Climatol.*, **57**, 1957–1975, https://doi.org/10.1175/JAMC-D-17-0340.1

2. Dörnbrack, A., S. Gisinger, N. Kaifler, T. C. Portele, M. Bramberger, M. Rapp, M. Gerding, J. Söder, N. Žagar, and D. Jelić, 2018: Gravity Waves excited during a Minor Sudden Stratospheric Warming, *Atmos. Chem. Phys*., **18**, 12915-12931, https://doi.org/10.5194/acp-18-12915-2018.

3. Egger, J. and Hoinka, K.-P., 2019: Hydrostatic vertical velocity and incompressibility in the Northern Hemisphere. *Q J R Meteorol Soc*., **145**, 563– 574. https://doi.org/10.1002/qj.3452

4. Fritts, D. C., S. B. Vosper, B. P. Williams, K. Bossert, M. J. Taylor, P.-D. Pautet, S. D. Eckermann, C. G. Kruse, R. B. Smith, A. Dörnbrack, M. Rapp, T. Mixa, I. M. Reid, and D. J. Murphy, 2018: Large-amplitude mountain waves in the mesosphere accompanying weak cross-mountain flow during DEEPWAVE Research Flight RF22. *Journal of Geophysical Research: Atmospheres*, **123**, 9992–10,022. https://doi.org/10.1029/2017JD028250

5. Rapp, M., A. Dörnbrack, and P. Preusse, 2018: Large midlatitude stratospheric temperature variability caused by inertial instability: A potential source of bias for gravity wave climatologies. *Geophysical Research Letters*, **45**, 10,682–10,690. https://doi.org/10.1029/2018GL079142

6. Sandu, I., A. van Niekerk, T. G. Shepherd, S. Vosper, A. Zadra, J. Bacmeister, A. Beljaars, A. Brown, A. Dörnbrack, N. McFarlane, F. Pithan, and G. Svensson, 2019: Orography and its impacts on the atmospheric circulation, *npj Climate and Atmospheric Science* **2**, Article number: 10. https://doi.org/10.1038/s41612-019-0065-9

7. Voigt, C., Dörnbrack, A., Wirth, M., Groß, S. M., Pitts, M. C., Poole, L. R., Baumann, R., Ehard, B., Sinnhuber, B.-M., Woiwode, W., and Oelhaf, H., 2018: Widespread polar stratospheric ice clouds in the 2015–2016 Arctic winter – implications for ice nucleation, *Atmos. Chem. Phys*., **18**, 15623-15641, https://doi.org/10.5194/acp-18-15623-2018.

8. Woiwode, W., Dörnbrack, A., Bramberger, M., Friedl-Vallon, F., Haenel, F., Höpfner, M., Johansson, S., Kretschmer, E., Krisch, I., Latzko, T., Oelhaf, H., Orphal, J., Preusse, P., Sinnhuber, B.-M., and Ungermann, J, 2018 Mesoscale fine structure of a tropopause fold over mountains, *Atmos. Chem. Phys*., **18**, 15643-15667, https://doi.org/10.5194/acp-18-15643-2018.

Summary of results

(1) Mesoscale fine structure of a tropopause fold over mountains (Woiwode et al. ACP 2018)

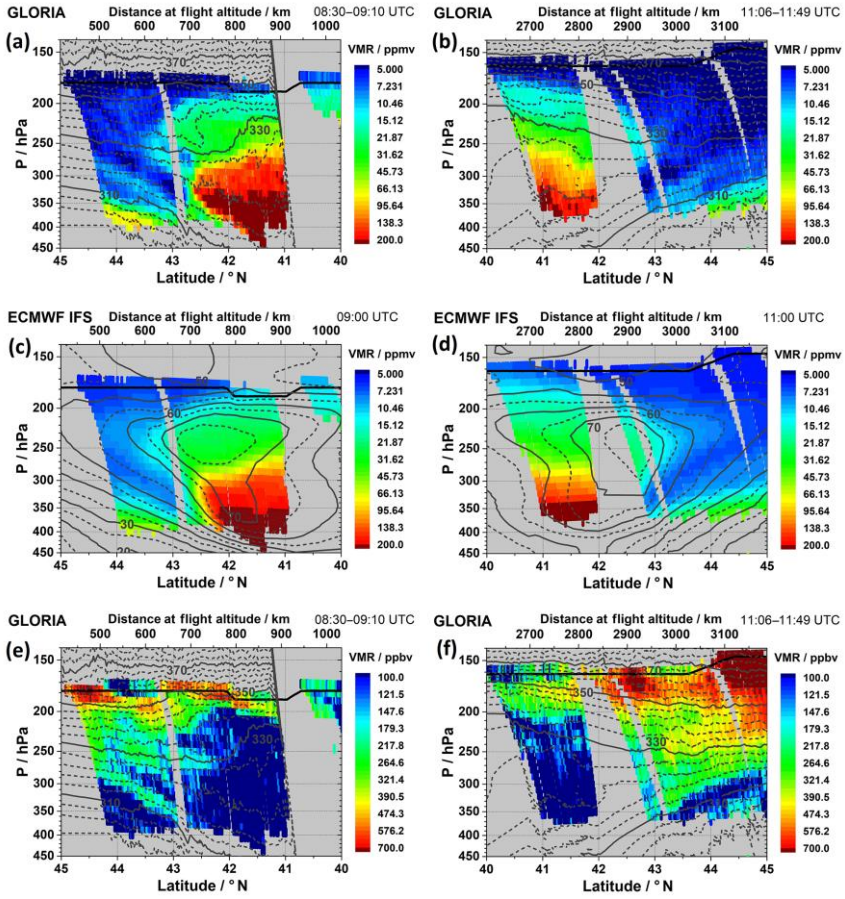

Figure 1: GLORIA observations of water vapour mixing ratio (a) and (b) and of ozone mixing ratio (e) and (f) for the southbound leg (left column) and the northbound leg (right column), respectively. Superimposed on panels (a), (b), (e), and (f) is potential temperature Θ (K, solid and dashed grey lines, $\Delta\Theta$ = 4 K) derived from GLORIA temperature observations and IFS HRES background pressure. Panels (c) and (d): IFS water vapour mixing ratio sampled using GLORIA observational filters. Horizontal wind V_H (m s^{-1}, solid and dashed grey lines, ΔV_H = 5 m s^{-1}) is superimposed on (c) and (d). Bold solid lines in all panels mark HALO's flight levels.

In this comprehensive case study, we report airborne remote-sensing observations of a tropopause fold during two crossings of the polar front jet over northern Italy on 12 January 2016. The GLORIA (Gimballed Limb Observer for Radiance Imaging of the Atmosphere) observations allowed for a simultaneous mapping of temperature, water vapour, and ozone. They revealed deep, dry, and ozone-rich intrusions into the troposphere. The mesoscale fine structures of dry filaments at the cyclonic shear side north of the jet and tongues of moist air entraining tropospheric air into the stratosphere along the anticyclonic shear side south of the jet were clearly resolved by GLORIA observations.

Vertically propagating mountain waves with recorded temperature residuals exceeding ±3 K were detected above the Apennines. Their presence enhanced gradients of all variables locally in the vicinity of the tropopause. The combination of H_2O–O_3 correlations with potential temperature reveals an active mixing region and shows clear evidence of troposphere-to-stratosphere and stratosphere-to-troposphere exchange.

High-resolution, short-term deterministic forecasts of ECMWF's integrated forecast system (IFS) applying GLORIA's observational filter reproduce location, shape, and depth of the tropopause fold very well (see Fig. 1). The fine structure of the mixing region, however, cannot be reproduced even

with the 9 km horizontal resolution of the IFS, used here. This case study demonstrates convincingly the capabilities of linear limb-imaging observations to resolve mesoscale fine structures in the upper troposphere and lower stratosphere, validates the high quality of the IFS data, and suggests that mountain wave perturbations have the potential to modulate exchange processes in the vicinity of tropopause folds.

(2) Hydrostatic vertical velocity and incompressibility in the Northern Hemisphere. (Egger and Hoinka, 2019)

The theoretical paper by Egger and Hoinka evaluates the vertical velocity w for the Northern Hemisphere from reanalysis data and two forms of the Richardson equation. This equation is based on the hydrostatic assumption and the thermodynamic energy equation. The standard form of the Richardson equation allows one to quantify the contributions to the vertical velocity of the horizontal divergence δ, the vertical pressure velocity ω and heating, and to test the incompressibility assumption underlying many dynamic models and theories. However, there are cancellations between two important terms. This shortcoming is substantially reduced in a further version of this equation where one term dominates. This version is the backbone of the data evaluation using ERA Interim.

The vertical velocities resulting from the Richardson equation in the troposphere are in good agreement with those obtained directly from the reanalysis data. It is found that the assumption of incompressibility provides a good estimate for w in the mid troposphere, even above Greenland and the Tibetan Plateau, both for the annual mean and the standard deviation of w, but is less acceptable in the upper troposphere and almost useless in the lower stratosphere. The contribution of heating to w is small.

(3) Gravity Waves excited during a Minor Sudden Stratospheric Warming (Dörnbrack et al. 2018)

An exceptionally deep upper-air sounding launched from Kiruna airport (67.82°N, 20.33°E) on 30 January 2016 stimulated the investigation of internal gravity waves excited during a minor sudden stratospheric warming (SSW) in the Arctic winter 2015/16. The analysis of the unique radiosonde profile revealed large kinetic and potential energies in the upper stratosphere without any simultaneous enhancement of upper tropospheric and lower stratospheric values. Upward propagating inertia-gravity waves in the upper stratosphere and downward propagating modes in the lower stratosphere indicated a region of gravity wave generation in the stratosphere. Two-dimensional wavelet analysis was applied to vertical time series of temperature fluctuations in order to determine the vertical propagation direction of the stratospheric gravity waves in one-hourly high-resolution meteorological analyses and short-term forecasts. The separation of up- and downward propagating waves provided further evidence for a stratospheric source of gravity waves.

A special feature of this study is the application of the MODES software developed by N. Zagar. This scale-dependent decomposition of the flow into a balanced component and inertia-gravity waves showed that coherent wave packets preferentially occurred at the inner edge of the Arctic polar vortex where a sub-vortex formed during the minor SSW (see, Fig. 2).

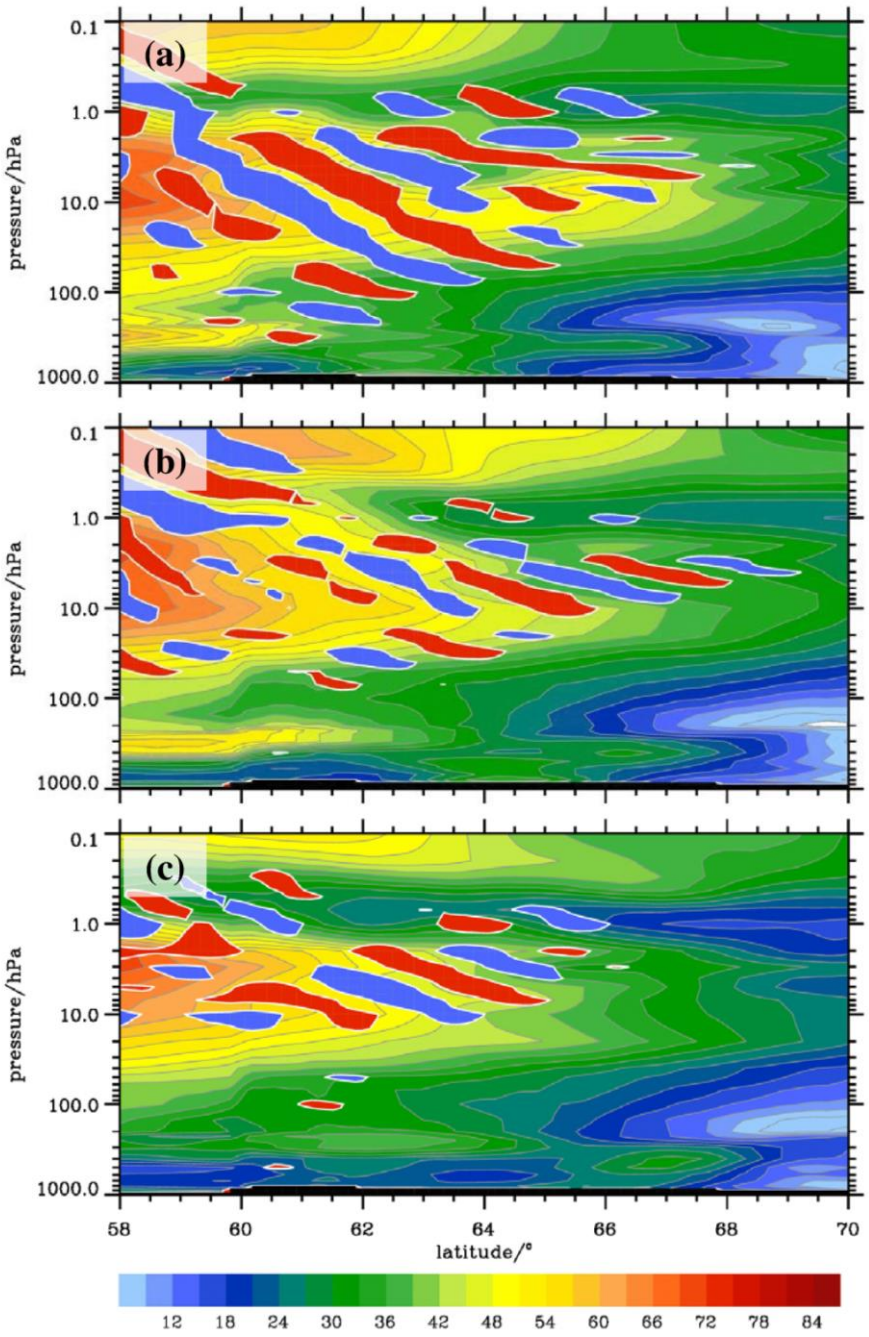

Figure 2: Composite of the magnitude of the balanced wind V_H^{BAL} (m s^{-1}, color shaded) and the unbalanced zonal wind U^{IGW} (areas with negative values larger -3 m s^{-1} and positive values smaller 3 m s^{-1} are filled with blue and red, respectively) from the normal mode analysis. The vertical sections are along the baseline sketched in Figs. 4 and 5 and they are valid on 30 January 2016 at 00 UTC (a), 06 UTC (b), and 12 UTC (c).

(4) Large midlatitude stratospheric temperature variability caused by inertial instability: A potential source of bias for gravity wave climatologies (Rapp et al. 2019)

Stratospheric temperature perturbations that have previously been misinterpreted as due to gravity waves are revisited. Usually, it is thought that such variations are caused by internal gravity waves that are excited by the vertical displacement of air. In the stably stratified stratosphere, these internal gravity waves are ubiquitous and constitute an important dynamical driver of stratospheric and mesospheric winds.

The stratospheric temperature perturbations observed by radio occultation during December 2015 had peak-to-peak amplitudes of 10 K extending from the equator to midlatitudes. The vertically stacked and horizontally flat structures revealed a vertical wavelength of 12 km. The signs of the stratospheric temperature perturbations were 180° phase-shifted between equatorial and middle latitudes at fixed altitude levels. High-resolution operational analyses reveal that these shallow temperature structures were caused by inertial instability due to the large meridional shear of the polar night jet at its equatorward flank in combination with Rossby wave breaking.

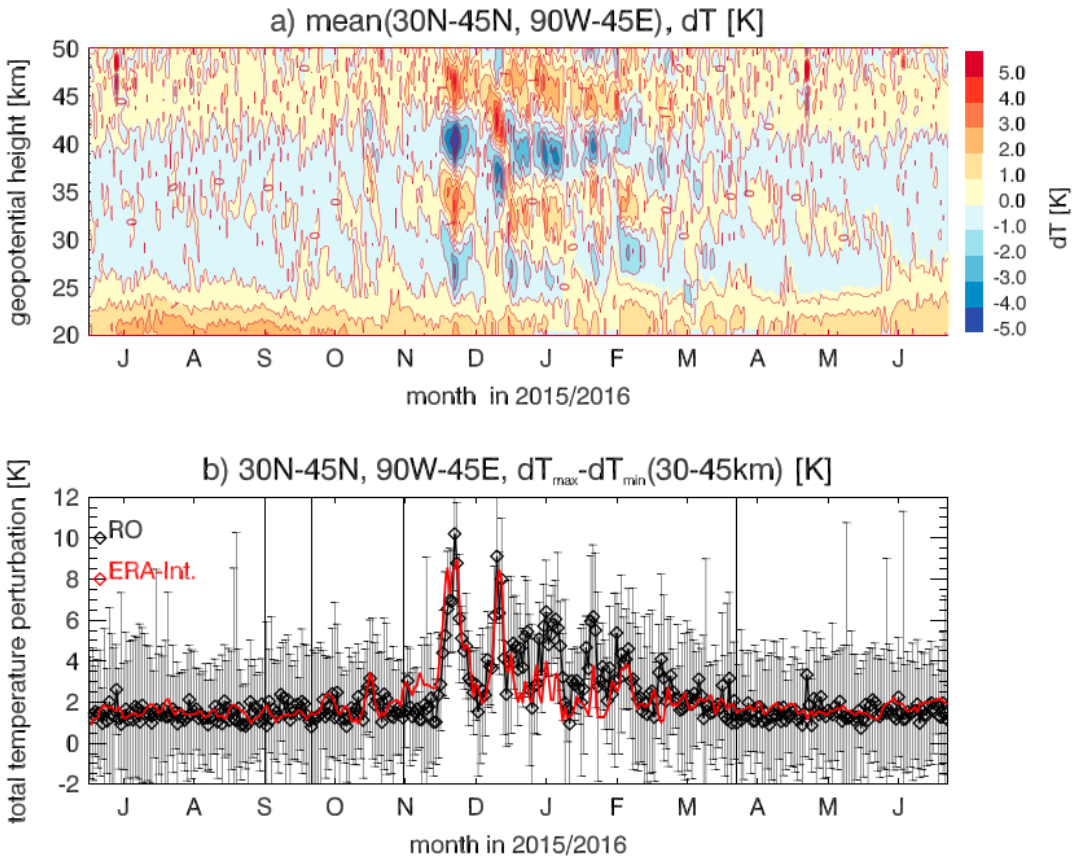

Figure 3: (a) Time series of daily mean stratospheric temperature perturbations versus altitude from METOP-A and METOP-B radio occultation data for the region 30–45∘N and 90∘W to 45∘E for the period from 1 July 2015 to 30 June 2016. Tick marks on the x axis indicate the 15th of each month. (b) Time series of total temperature perturbation (maximum-minimum perturbation) between 30 and 45-km altitude in the time series shown in panel (a), in black, along with corresponding error bars. The red line indicates corresponding total stratospheric temperature perturbations from ERA-Interim for the same location and time. RO = radio occultation; ERA-Interim = ECMWF Re-Analysis-Interim.

Large stratospheric temperature perturbations owing to inertial instability do frequently occur in the Northern Hemisphere (Southern Hemisphere) from October to April (April to October) in the 39 years of ECMWF Re-Analysis-Interim data (see, Fig. 3). During 10% of the days, the stratospheric temperature perturbations exceed 5 K (peak to peak). Our results are important for properly constructing gravity wave climatologies (where inertial instability events must be excluded) — which are in turn an important input for the correct formulation of global circulation models**.**